JOURNAL OF GUIDANCE, CONTROL, AND DYNAMICS
Vol. 29, No. 2, March–April 2006

Design of a Gain-Scheduled Flight Control System Using Bifurcation Analysis

Thomas Richardson,* Mark Lowenberg,† Mario diBernardo,‡ and Guy Charles§
University of Bristol, Bristol, England BS8 1TR, United Kingdom

A method for identifying regions of instability in closed-loop systems has been developed for flight dynamics applications. This forms a novel approach in which a surface of equilibria is generated in the region of interest as the influence of the control system is increased. In this way, the creation and destruction of equilibria in the controlled system can be easily found and visualized. This systematic approach allows the stability of the closed-loop system to be directly related to that of the open loop. Results are given for a highly nonlinear aircraft model and demonstrate the power of a combined analytical and graphical approach to control system synthesis.

I. Introduction

IN recent years, there has been significant interest in the application of nonlinear analysis methods to flight dynamics problems.[1–3] These methods have been applied to many fields to predict and describe the evolution of nonlinear systems over wide variations in parameters, for example, in voltage collapse[4] and macroeconomic systems.[5] The application to flight dynamics was initiated by Mehra et al. in 1977.[6] However, the vast majority of all published work has been for the bifurcation analysis of unaugmented aircraft, or aircraft with simple stability augmentation systems.

Feedback control systems are used to augment the response of the aircraft in regions where the open-loop behavior is undesirable. The ongoing requirement to increase the performance of modern aircraft necessitates stretching the flight envelope into highly nonlinear regions, such as those at a high angle of attack. One simple approach to improve the aircraft response is to use a fixed linear controller generated at a given operating point. In many cases, however, this is insufficient, and the aircraft may still display unacceptable handling qualities. The logical extension of this approach is to schedule the control system gains.

Gain scheduling is a practical method of coping with known plant nonlinearities. Here we define gain scheduling as the process of varying a set of controller coefficients according to the current value of a scheduling signal. Conventional gain scheduling is carried out by taking linearizations of the nonlinear plant at a few selected points in the system's operating range. Subsequently, either the model linearizations or resultant controller gains are scheduled between the design points by using simple interpolation methods. Recently, gain-scheduling and linear parameter-varying (LPV) systems have been the basis of a great deal of research,[7] and the application of gain scheduling to nonlinear systems continues to present interesting research problems.

Continuation methods are the established tools that underlie the application of bifurcation analysis to nonlinear systems; they are path-following algorithms that trace out solutions to nonlinear algebraic equations, in this case steady states of the open- or closed-loop flight dynamics model. We believe that there is great deal of potential in the use of continuation methods in the design and analysis of gain-scheduled feedback control systems. They allow us to address systems with significant nonlinearity and in particular multivalued steady states. The essence of this paper is to consider the application of a gain-scheduled state feedback controller to an aircraft. Continuation algorithms are used for two purposes within this paper: 1) to create pseudocontinuous gain schedules throughout a wide operating region and 2) to create surfaces of state equilibria that show changes in the global behavior of the system ranging from the open-loop to the closed-loop configurations.

The first step in this approach is to create pseudocontinuous gain functions that satisfy the design criteria at equilibrium throughout the desired operating region of the nonlinear system. Given sufficient control authority, these allow the dynamic response of the desired branch of equilibria to be specified. This paper formalizes a continuation approach to gain scheduling using standard feedback control design terminology.

The second step is to determine the global implications of this gain-scheduled controller. A novel approach is adopted in which three-dimensional bifurcation surfaces of equilibria are found as both the reference signal and the controller gains are varied. This powerful technique illustrates graphically the influence of the control system and is shown to be invaluable in the evaluation of the global stability of the system. These bifurcation surfaces can be used to indentify undesired attractors within the closed-loop system. The creation of equilibrium surfaces in terms of the variation in control system gain is an entirely new concept in aircraft controller design and allows a tradeoff between local and more global properties of the closed-loop system.

These methods are demonstrated using a highly nonlinear aircraft model, the hypothetical high angle of incidence research model (HHIRM).[8] Aircraft dynamics are complex, incorporating nonlinearities as a result of many factors such as inertial coupling between the different degrees of freedom and aerodynamic forces and moments.[9]

An important problem is to understand and characterize the robustness of the control strategy to unwanted perturbations, model uncertainty, and variability and unmodeled dynamics. As discussed in the paper, we believe continuation methods can be used to investigate the robustness properties of the controller of interest. For example, their use in Sec. VI to study the sensitivity of the control design process to parameter variation could equally have been applied to parametric uncertainties. Nevertheless, we wish to emphasize here that the precise role that bifurcation analysis can play in understanding and characterizing the robustness of a given control strategy is still an open problem that is currently being debated in the nonlinear dynamics and control community (for instance, Ref. 10) and is, therefore, beyond the scope of the paper.

The paper is organized as follows. The objective and the design approach are given in Sec. II. Section III contains descriptions of the

Received 11 October 2004; revision received 18 March 2005; accepted for publication 21 March 2005.

*Lecturer, Department of Aerospace Engineering, Queens Building; thomas.richardson@bristol.ac.uk. Member AIAA.

†Senior Lecturer, Department of Aerospace Engineering, Queens Building. Senior Member AIAA.

‡Reader, Department of Engineering Mathematics, Queens Building.

§Ph.D. Student, Department of Mechanical Engineering, Queens Building.

control design and analysis methods. The aircraft model considered is presented in Sec. IV. Open- and closed-loop bifurcation analysis results are given in Sec. V. In Sec. VI, continuation is applied to normalized control system parameters. Conclusions are given in Sec. VII.

II. Objective and Design Approach

The objective is to find a set of commanded steady states that have corresponding desired dynamic properties throughout a specified parameter range. We assume that desired steady states will be equilibria (trim points). In the aircraft application considered here, the desired equilibria are defined by a relationship between a member of the state vector and an input parameter, that is, by prescribing a projection of the bifurcation diagram, in this case angle of attack α, vs desired reference input r. For simplicity, we choose r to be commanded α, so that graphically this relates to a unique set of trim points that have a linear relationship between the reference signal and the α state. Note that the control systems used in this work are not intended to be ideal solutions but have been selected to illustrate the power of using continuation methods in control system design.

A scheduled feedforward term may be used alone to create a linear relationship between the demanded reference signal and a chosen system state. Although guaranteeing that the resulting system will exhibit a desired set of equilibria, in general, these will not be stable or unique. The bifurcation diagrams reported in our example will show that this is indeed the case with the system exhibiting several coexisting equilibria at the same parameter values. Hence, the resulting demanded trim points are shown to exist without being necessarily stable and, in the case in point, intersect with additional undesired branches of equilibria.

Desired stability is obtained using closed-loop feedback control. The scheduled feedforward term is augmented with a scheduled set of feedback gains generated via a novel implementation of continuation and eigenstructure algorithms. This implementation is shown to result in a linear branch of trim points with the desired local stability. Globally, however, simulation results and bifurcation diagrams for the HHIRM indicate the presence of an isola, a set of of stable and unstable trim points (forming a closed branch in the bifurcation diagrams) that influence the global transient response of the augmented aircraft.

To illustrate graphically the origin of this isola, a further novel implementation of continuation algorithms is made. The smooth nonlinear functions of the control system gains are multiplied by a scaling factor Λ, which is then used as the continuation parameter to generate a bifurcation or equilibrium surface. To generate these results, it is necessary to recalculate the nonlinear feedforward function at each point in the continuation to create the desired linear relationship between the reference input and the selected state. The results show graphically the transition from open loop to closed loop and identify the origin and evolution of the isola in the closed-loop system as the feedback schedules are scaled in magnitude. This provides a means of establishing the effect of changes in feedback schedule on both the local eigenstructure and the global dynamics.

To remove the unwanted isola in the closed-loop system, an integral term is introduced, and the resulting closed-loop bifurcation diagrams are shown to contain only the single stable desired branch. Therefore, given sufficient control authority, it is shown to be possible to create a single stable attactor within the desired operating region.

The methods described in this section are presented analytically in the next section and form a logical, systematic approach to control system design. They are shown to give insight into, and understanding of, complex, highly nonlinear aircraft models.

III. Control System Design

A. Bifurcation Analysis

An introduction to the geometrical analysis of nonlinear systems and bifurcations can be found, for example, by Strogatz.[11] Crucially, bifurcation analysis and bifurcation diagrams allow a global view of nonlinear systems, which is not possible by simply analyzing the system at a few given design points. This is important for many engineering systems that operate over wide envelopes with highly nonlinear regions. Two examples of such systems are aircraft and chemical mixing processes.[1–3,12]

Consider the nonlinear system given by

$$\dot{\boldsymbol{x}} = \boldsymbol{f}(\boldsymbol{x}, u) \qquad \boldsymbol{x} \in \Re^n, \qquad u \in \Re \tag{1}$$

where $\boldsymbol{x}$ is the state vector and u is the control input of interest (others considered fixed, with no loss of generality) and $\boldsymbol{f}$ is a smooth nonlinear vector field.

Bifurcation analysis is carried out to find the open-loop equilibria (or fixed points) $\bar{\boldsymbol{x}}$ as the control input is varied quasi statically in a range of interest, that is, solutions to

$$\dot{\boldsymbol{x}} = \boldsymbol{f}(\bar{\boldsymbol{x}}, \bar{u}) = 0, \qquad \bar{\boldsymbol{y}} = \boldsymbol{g}(\bar{\boldsymbol{x}}) \tag{2}$$

where $\bar{\boldsymbol{x}}$ is the state equilibrium, not necessarily stable, corresponding to input $\bar{u}$. Bifurcation analysis often involves generating paths of periodic orbit solutions, in addition to those of the fixed points; these are not required for the purposes of this paper.

Given a suitable starting point, numerical continuation software can be used to solve for a branch of equilibria as u is varied. The information can be plotted graphically as a bifurcation diagram,[11] which is used to predict the global dynamics of the nonlinear system; (for example, see Fig. 1).

Continuation methods make use of the implicit function theorem,[13] which implies that Eq. (2) defines implicitly a smooth

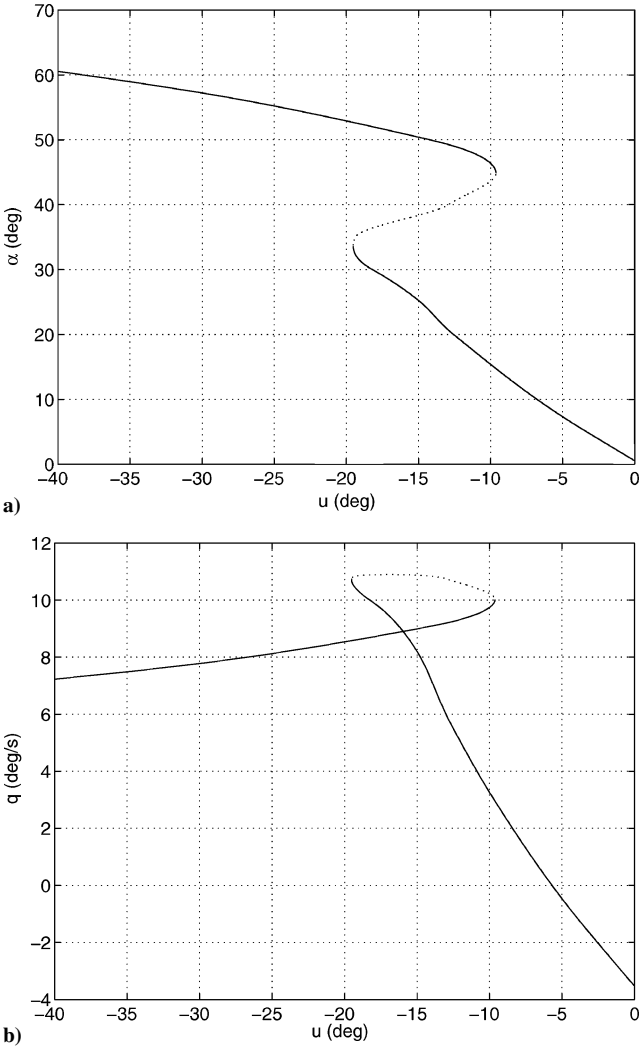

Fig. 1 Open-loop bifurcation diagrams: ——, stable equilibria and – – –, unstable.

nonlinear relationship between state and input, namely, $\bar{\boldsymbol{x}} = \boldsymbol{\eta}(\bar{u})$. Therefore, $\bar{y}$ can be expressed in terms of $\bar{u}$ as

$$\bar{y} = \gamma(\bar{u}) \tag{3}$$

where $\bar{y}$ relates to a single output and throughout this work to the actual aircraft angle of attack. These functions can be created as a set of discrete tabulated data by using continuation software such as AUTO.[14] Note that continuation methods can be used to solve for equilibria of the system throughout the whole range of the control input.

The implementation of continuation algorithms has been expanded to incorporate the calculation of control system gains, using eigenstructure assignment in this case, for every desired equilibrium point as the continuation parameter is varied. In a smooth nonlinear system, this results in a smooth set of nonlinear gain functions that can be scheduled against a chosen parameter. Care needs to be taken in the choice of this scheduling parameter to avoid introducing additional dynamics in the form of undesired hidden coupling terms.

B. Control System Structure

Initially a control system will be considered that consists of two elements.

The first is a nonlinear scheduled feedforward signal $u_{\text{ff}} = \phi(r)$ such that there exists a (not necessarily unique or stable) set of equilibria $(\bar{\boldsymbol{x}}, \bar{\boldsymbol{y}})$, throughout the desired range of r (the reference input), where

$$\bar{y} = \bar{r} \qquad \forall \quad \bar{r} \in (r_{\min}, r_{\max}) \tag{4}$$

which is a subset of the equilibria defined by

$$\dot{\boldsymbol{x}} = \boldsymbol{f}(\bar{\boldsymbol{x}}, \bar{u}) = 0 \tag{5}$$

$$\bar{\boldsymbol{y}} = \boldsymbol{g}(\bar{\boldsymbol{x}}) \tag{6}$$

The second element is a nonlinear feedback signal u_{fb}, gain scheduled throughout the desired range of r, such that only the set of equilibria described by Eq. (4) exists and that they are asymptotically stable and locally exhibit a desirable transient response. The specific approach taken here is to assign the response in terms of the eigenstructure of the system at equilibrium.

C. Feedforward Control

Figure 2 is a schematic block diagram showing a simple feedforward control system. In this case, the input to the plant is defined as a nonlinear function of the reference input r. This control implementation allows an input-to-output relationship to be established but cannot be used to define the stability of the resulting system. To generate a set of output equilibria as a direct function of the reference, considering Eq. (3), we choose

$$\bar{u} = u_{\text{ff}} = \gamma^{-1}(\bar{r}) = \phi(\bar{r}) \tag{7}$$

where u_{ff} is the feedforward control signal as in Fig. 2. Substituting Eq. (7) into Eq. (3) reveals that

$$\bar{y} = \gamma(\bar{u}) = \gamma[\gamma^{-1}(\bar{r})] = \bar{r} \tag{8}$$

throughout the range of the reference, r. The equilibria formed at $\bar{y} = \bar{r}$ will not necessarily be stable or unique, depending on the nature of the nonlinear function γ. If γ describes unstable equilibria, then the feedforward controlled continuation will exhibit corresponding unstable equilibria.

The method of finding the feedforward signal u_{ff} already described relies on the open-loop function $\gamma(\bar{r})$ being invertible. Because the function γ is found numerically using continuation software, γ is available as a set of data points along the branch of

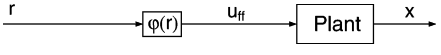

Fig. 2 Feedforward control.

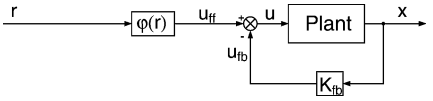

Fig. 3 State feedback plus feedforward control.

equilibria. The numerical inversion of γ is achieved by simply interpolating the data from $\bar{y}$ to $\bar{u}$.

A problem arises if after continuation γ is found to be a many-to-one function, that is, more than one value for $\bar{u}$ corresponds to many values of $\bar{y}$. Here, the (numerical) inversion of γ is impossible because we cannot find one value of u to achieve a single desired value of y. However, the inversion is possible if the function is one-to-many, as will be demonstrated in the aircraft example in Sec. V.

The approach to take if γ is many-to-one is to take the principal branch of the equilibria: using part of the numerical data for the inversion at a time. This may require the implementation of a piecewise approach to move between several different scheduled areas of the bifurcation diagram, but such is the nature of nonlinear systems it would be impossible to cover all of the possibilities here. Suffice to say that a level of practicality would need to be employed in the final controller design to ensure desired closed-loop system behavior.

D. Feedforward and Feedback Control

Now we synthesize the control input u as consisting of two actions (as in Sec. III.B and as shown in Fig. 3),

$$u = u_{\text{ff}} + u_{\text{fb}} \tag{9}$$

A state feedback action is chosen of the form

$$u_{\text{fb}} = \boldsymbol{K}_{\text{fb}}\boldsymbol{x} \tag{10}$$

We shall seek to schedule the gains $\boldsymbol{K}_{\text{fb}}$ by making explicit use of continuation methods. In so doing, $\boldsymbol{K}_{\text{fb}}$ will be found as a function of u_{ff} and in turn of r, allowing $\boldsymbol{K}_{\text{fb}}$ to be scheduled throughout the flight envelope. The feedforward control u_{ff} will then be synthesized in terms of r in a similar manner to that described in the preceding section.

Note that it is also possible to calculate the feedback gains to operate on the state error $(\boldsymbol{r} - \boldsymbol{x})$, where $\boldsymbol{r}$ would be the full reference vector, thus designing the controller about the equilibria already defined by the feedforward control. If this is done, then there is no need to recalculate the feedforward control term. The drawback though is that there is an increase in the number of scheduled terms required, including the full set of states at equilibrium, $\bar{\boldsymbol{x}}$.

For the results generated in this paper, the feedback gains operate on the system state vector $\boldsymbol{x}$. Even though this requires a recalculation of the feedforward function during the synthesis process, the overall result is a reduced set of scheduled terms. These terms can either be scheduled against the continuation parameter r (which represents the stick position) and/or uncoupled states. Scheduling against closely coupled terms (such as α and q) can result in hidden coupling terms and undesired dynamics.

It is possible to account for some of these hidden coupling terms and to schedule against closely coupled system states.[15] The required transformation relies on the smooth, continuous variation of the gains with system states and results in a controller that is closer to ideal for the current state of the system. For the purposes of this paper, the feedback gains are scheduled against desired states and, therefore, the reference input r.

E. Gain Scheduling

The standard approach to gain scheduling for a nonlinear system is to take linearizations at several design points throughout the desired operating region,

$$\delta\dot{\boldsymbol{x}} = \left.\frac{\partial \boldsymbol{f}(\boldsymbol{x}, u)}{\partial \boldsymbol{x}}\right|_i \delta\boldsymbol{x} + \left.\frac{\partial \boldsymbol{f}(\boldsymbol{x}, u)}{\partial u}\right|_i \delta u \tag{11}$$

where i represents the evaluation at the ith design point and $\delta \boldsymbol{x}$ and δu are perturbations in the system from the design point.

A linear control strategy can be implemented using the linearized system to achieve the desired closed-loop characteristics. Gain scheduling is performed between the design points by interpolating the gains to effect a smoothly varying set of gains throughout the range of r.

Note that selecting suitable design points is not a trivial task. The nature of wide parameter-varying nonlinear systems is such that between design points the system dynamics may vary significantly and, thus, have a detrimental effect on the closed-loop response.

F. Pseudocontinuous Gain Scheduling

To select a set of feedback gains $\boldsymbol{K}_{\text{fb}}$ that guarantees the desired closed-loop dynamic properties, eigenstructure assignment was integrated within the continuation algorithm. This novel implementation of eigenstructure assignment places the closed-loop poles of the linearized system during continuation and along the entire branch of equilibria.

From Eq. (2) the controlled system is given by

$$\dot{\boldsymbol{x}} = \boldsymbol{f}(\boldsymbol{x}, u_{\text{ff}} + \boldsymbol{K}_{\text{fb}}\boldsymbol{x}) = \boldsymbol{h}(\boldsymbol{x}, u_{\text{ff}}, \boldsymbol{K}_{\text{fb}}), \qquad \boldsymbol{y} = \boldsymbol{g}(\boldsymbol{x}) \tag{12}$$

The eigenstructure assignment and calculation of the equilibria are carried out at the same time by applying continuation to the following set of equations (using u_{ff} as the continuation parameter). Continuation can be just as easily carried out letting $y = r$ and using r as the continuation parameter. This would solve for the feedforward control u_{ff} and the feedback gain $\boldsymbol{K}_{\text{fb}}$ in one step. The process is laid out in two steps here for clarity,

$$\boldsymbol{h}(\boldsymbol{x}, u_{\text{ff}}, \boldsymbol{K}_{\text{fb}}) = 0, \qquad (\boldsymbol{A} - \boldsymbol{B}\boldsymbol{K}_{\text{fb}})\boldsymbol{v}_i^d = \boldsymbol{\lambda}_i^d \boldsymbol{v}_i^d \tag{13}$$

where $\boldsymbol{A}$ and $\boldsymbol{B}$ relate to the linearized system at each step in the iteration and are defined by

$$\boldsymbol{A} = \frac{\partial \boldsymbol{f}(\boldsymbol{x}, u)}{\partial \boldsymbol{x}}, \qquad \boldsymbol{B} = \frac{\partial \boldsymbol{f}(\boldsymbol{x}, u)}{\partial u} \tag{14}$$

and the eigenstructure is assigned through the set of n self-conjugate distinct desired complex eigenvalues of the linearized closed-loop system, $\boldsymbol{\lambda}_i^d$, $i = 1, 2, \ldots, n$, and the n distinct desired eigenvectors of the linearized closed-loop system, $\boldsymbol{v}_i^d$, $i = 1, 2, \ldots, n$.

Note that even if there is a solution to the eigenstructure problem the solution has to be interpreted in light of the real-life nonlinear application. For example, large gains will lead to actuator and control surface saturation. From Eq. (13), the implicit function theorem allows us to express the output equilibria and scheduled feedback gains as

$$\bar{y} = \phi(u_{\text{ff}}) \tag{15}$$

$$\boldsymbol{K}_{\text{fb}} = \psi(u_{\text{ff}}) \tag{16}$$

which can be found numerically using continuation software such as AUTO.

Note that this approach is fundamentally different from conventional eigenstructure assignment,[16] where the method is used to place the eigenvalues of the linearized system around a predetermined finite set of operating conditions. This traditional gridded approach can give rise to difficulties when, for example, the nonlinear system changes topological form between the selected points via a fold bifurcation: The designer does not have a clear understanding of the evolution of underlying system behavior as parameters vary. Problems may then be encountered in trimming the system, and the control solution, if achieved, may differ substantially from that at a neighboring design point. In this novel approach, however, the eigenstructure assignment is carried out within the continuation algorithm and during iteration for the equilibria, thus overcoming some of these difficulties.

G. Feedforward Schedule

Feedback control as given in the preceding section is used to alter the dynamic properties of the closed-loop system, and feedforward control is used to generate a desired relationship between the reference input and output of the system.

We can now design the feedforward action from Eq. (15). As in Sec. III.C for designing u_{ff} in the absence of feedback control, we define the nonlinear feedforward schedule as

$$u_{\text{ff}} = \phi^{-1}(\bar{r}) \tag{17}$$

to ensure that $\bar{y} = \phi[\phi^{-1}(\bar{r})] = \bar{r}$. Therefore, from Eqs. (16) and (9), the complete control strategy will be

$$\boldsymbol{K}_{\text{fb}} = \psi[\phi^{-1}(\bar{r})] \tag{18}$$

$$u = \phi^{-1}(\bar{r}) + \psi[\phi^{-1}(\bar{r})]\boldsymbol{x} \tag{19}$$

IV. HHIRM Aircraft Model

The HHIRM[8] was created to provide a benchmark for nonlinear analysis and control design. The aerodynamic characteristics of the HHIRM are very similar to those of many existing combat aircraft and can be easily tuned to arbitrarily chosen characteristics for qualitative nonlinear dynamics analysis and control law design.

The HHIRM is ideal for research into control law design because the aerodynamic and thrust models are based entirely on analytical functions of aircraft parameters. All of these functions are smooth, and therefore, it is implicit that within the specified control surface limits the model may be highly nonlinear but remains smooth. The use of mathematical functions instead of large unwieldy aerodynamic tables means that the resulting computer code for the entire model is far smaller and faster to run. A second-order implementation of the HHIRM is used in this paper to illustrate the methodology; it describes the approximate short-period longitudinal dynamics

$$\dot{\alpha} = q + Z_w(\alpha, u)/mV_T, \qquad \dot{q} = M(\alpha, u)/I_{yy} \tag{20}$$

where

α	=	angle of attack
q	=	body axis pitch rate
u	=	system input (elevator deflection)
m	=	mass
V_T	=	total velocity
I_{yy}	=	y body axis moment of inertia

$M(\alpha, u)$ and $Z_w(\alpha, u)$ are the body axis pitching moment and force normal to the wind axis respectively, due to the aerodynamics, thrust, and gravity.

The difficulty in the control of the HHIRM arises from the highly nonlinear aerodynamic forces and moments that exist at high angles of attack. These are evident even in this simple reduced version of the model in the form of multiple attractors at certain values of u.

Several different aircraft control configurations can be used such as pitch rate or normal acceleration demand systems. For simplicity, in this paper, an α demand system is used throughout; in the following examples, α will be taken as the controlled output.

The control objective is for the aircraft to exhibit a steady-state value $(\bar{\alpha}, \bar{q})$ characterized by $\bar{\alpha} = \bar{r}$. Moreover, the aircraft must also achieve level-1 short-period handling qualities, which can be shown to be associated with eigenvalues of the system Jacobian matrix (see Refs. 17 and 18). We choose the desired eigenvalues to be

$$\lambda^d = -2.0 \pm 2.0j \tag{21}$$

V. Initial Results

A. Baseline Aircraft Analysis

The steady-state values of α and q were found for the baseline HHIRM under variation of the control input u, the elevator, that is, using the continuation methods described in Sec. III.A to solve for equilibria with u as the continuation parameter.

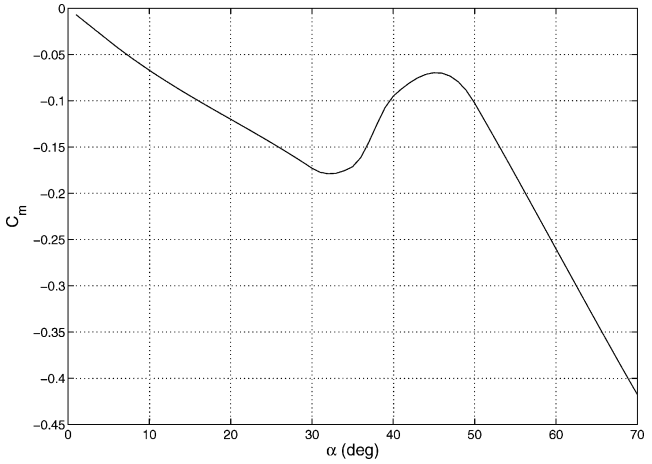

Fig. 4 C_m vs α, where $u = 0$.

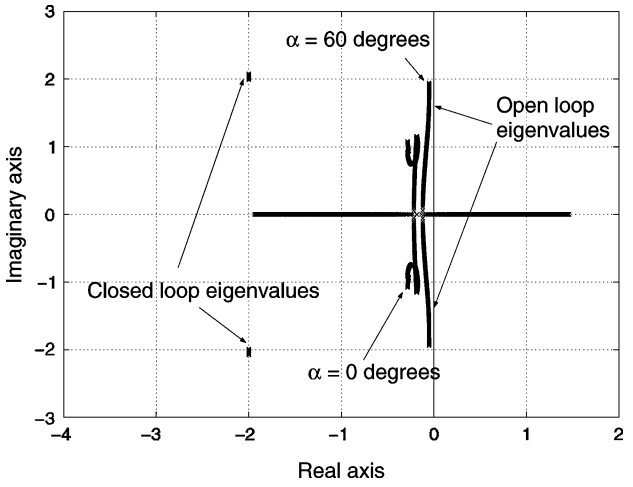

Fig. 5 HHIRM open- and closed-loop eigenvalues.

Figure 1 shows the equilibria set for both α (Fig. 1a) and q (Fig. 1b) against the continuation parameter u. The single branch has two folds at $(\bar{\alpha}, \bar{u}) = (33.8, -19.8)$, $(45.5, -9.5)$ deg, where a single real eigenvalue crosses the imaginary axis. The folds correspond to the onset of a family of unstable equilibria where the aircraft experiences a loss of pitch stiffness. This is verified by reference to the variation of C_m with α in Fig. 4: Static stability ($C_{m_\alpha} < 0$) is lost at $\alpha = 33.8$ deg, corresponding to the first fold in the bifurcation diagram and associated loss of stability; it is then regained at $\alpha = 45.5$ deg, giving rise to the second fold and the ensuing asymptotically stable deep stall situation evident up to $\alpha \approx 60$ deg. Note that the two folds cause a hysteresis effect: The pilot can switch between the low-to-moderate incidence stable behavior and the very high incidence stable branch, but only by moving the elevator past the relevant critical value for each fold.

The set of equilibria for the controlled output, $\bar{\alpha}$, along the branch can be expressed numerically as a nonlinear function of the control input $\bar{u}$,

$$\bar{\alpha} = \gamma_{ac}(\bar{u}) \tag{22}$$

The corresponding eigenvalues of the Jacobian matrix of the open-loop system are given in Fig. 5. They show that, even where the aircraft is stable, the system exhibits undesirable longitudinal handling qualities in terms of damping ratio and undamped natural frequency.

Carrying out bifurcation analysis of the uncontrolled system in this way generates a wealth of useful information on the behavior of the system, which in turn can help the controller design, especially in high-order asymmetric systems with multiple solution branches and changes in stability.

B. Feedforward Control

To demonstrate graphically the effect of feedforward control alone, the system is modified by substituting

$$u_{\text{ff}} = \gamma_{ac}^{-1}(\bar{r}) \tag{23}$$

into Eq. (20), and Fig. 6 shows the numerical function γ_{ac}^{-1}.

Figure 7 contains the bifurcation plots for the HHIRM with feedforward control. In this case, r is used as the continuation parameter.

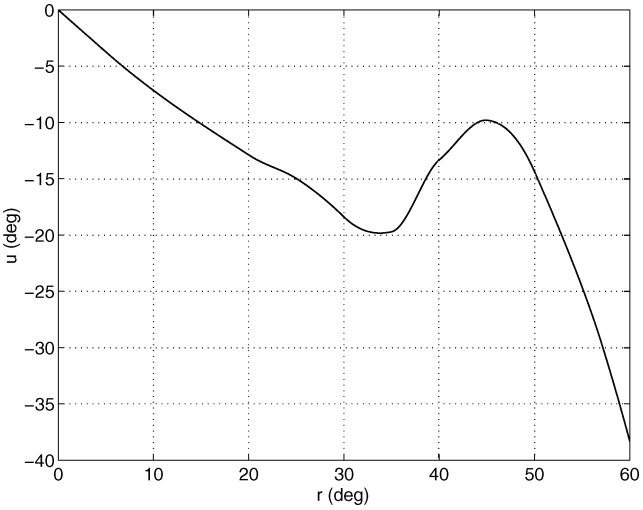

Fig. 6 Nonlinear feedforward function γ_{ac}^{-1}.

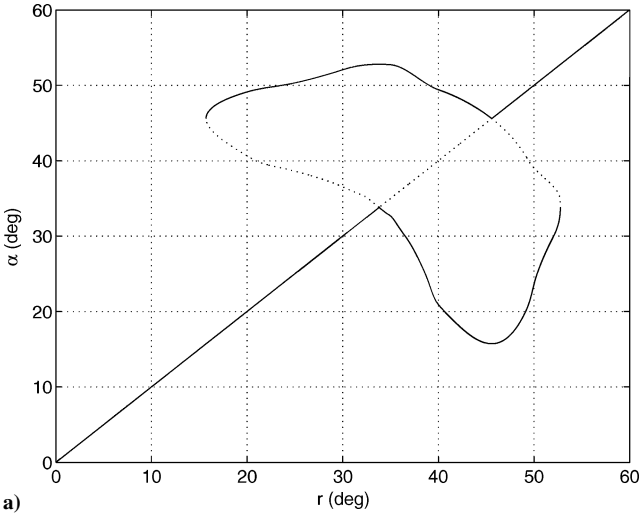

a)

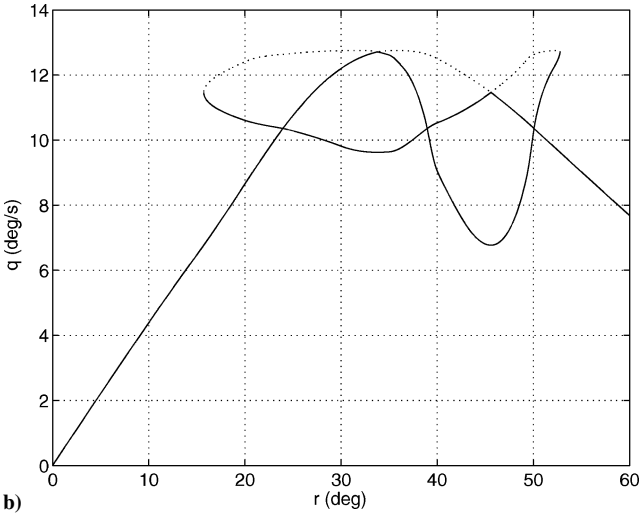

b)

Fig. 7 Bifurcation diagrams: aircraft with feedforward control.

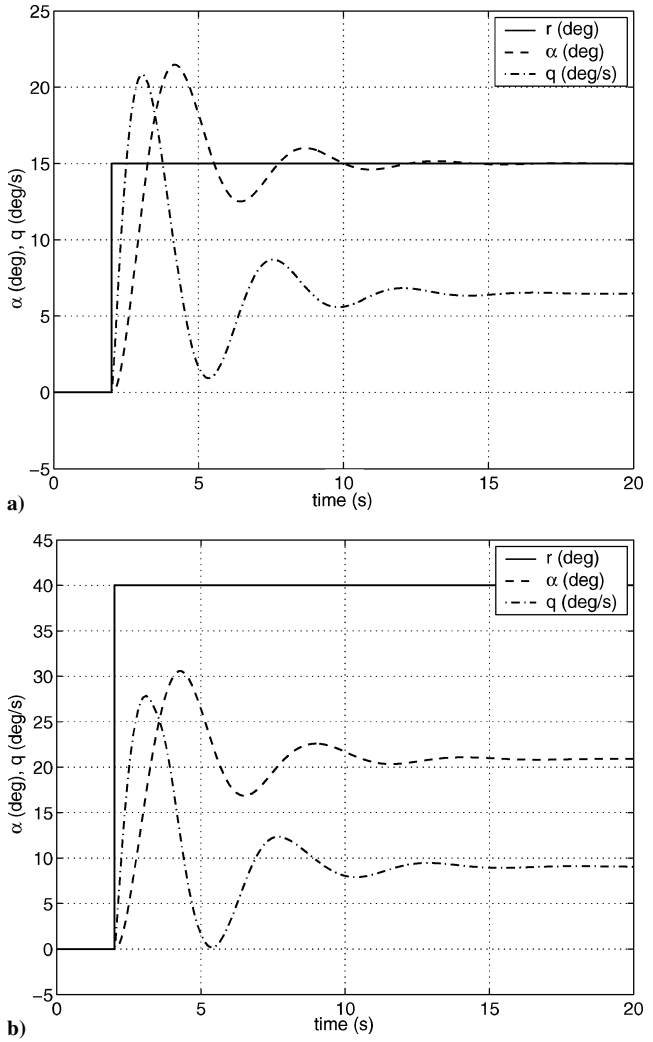

Fig. 8 HHIRM response under feedforward control: a) 15-deg step in *r* and b) 40-deg step in *r*.

Note that the reference set of equilibria $\bar{\alpha} = \bar{r}$ exists; however, there is an unstable section in the branch and there are coexisting branches of equilibria linked to the desired branch at two transcritical bifurcations. Note also that the unstable equilibria correspond to the unstable region in Fig. 1 ($33.8 < \bar{\alpha} < 45.5$ deg).

Figure 8 shows the response of the HHIRM to two step changes in the input r, starting at $r = 0$. The response to a 15-deg step settles down onto the desired equilibrium; however, the response to the 40-deg step demand settles onto a coexisting equilibrium (whose existence is predicted in the feedforward bifurcation diagram, Fig. 7). In both cases, the system is underdamped, and the dynamic response is highly undesirable.

The implication is that feedback control should be used to address these issues, that is, to 1) stabilize the unstable branch, 2) improve the transient response, and 3) suppress the coexisting attractors or reduce their basins of attraction. This latter task would be particularly important because the presence of coexisting attractors will undermine the control robustness to unwanted perturbations and noise. Thus, it would be desirable, once coexisting attractors have been located via bifurcation analysis, to be able to assess their regions of attraction. This is still an open problem in nonlinear dynamics and, currently, only heuristic or brute force numerical methods can be used for such an estimation. For example, cell-mapping methods[19] can be used to estimate numerically the basin of attraction of a given solution but were found to give inaccurate results for high-dimensional dynamical systems or in the case of many coexisting attractors. A detailed analysis of the regions of attraction is currently under development but is beyond the scope of this paper.

C. Feedforward and Feedback Control

The feedforward and feedback control signal is given by:

$$u = u_{\text{ff}} + K_\alpha \alpha + K_q q \tag{24}$$

When u_{ff} is used as the continuation parameter, eigenstructure assignment is carried out within the continuation algorithm; thus, the numerical information for the output α and gains K_α and K_q may be expressed as

$$\bar{\alpha} = \phi_{ac}(u_{\text{ff}}) \tag{25}$$

$$K_\alpha = \psi_{ac_\alpha}(u_{\text{ff}}) \tag{26}$$

$$K_q = \psi_{ac_q}(u_{\text{ff}}) \tag{27}$$

As in the preceding section, the feedforward schedule is now formed as $u_{\text{ff}} = \phi_{ac}^{-1}(\bar{r})$, and it is shown in Fig. 9.

The feedback gains can, therefore, be constructed as

$$K_\alpha = \psi_{ac_\alpha}\left[\phi_{ac}^{-1}(r)\right] \tag{28}$$

$$K_q = \psi_{ac_q}\left[\phi_{ac}^{-1}(r)\right] \tag{29}$$

In Fig. 10, the two gains K_α and K_q have been plotted against r. The gain that remains relatively constant is K_q, and the second, which demonstrates highly nonlinear behavior at high r (corresponding to high α), is K_α. This is as expected due to the response of the baseline aircraft being linear at low angles of attack and substantially nonlinear at higher incidence, in particular for α between 30 and 50 deg (Figs. 1 and 4).

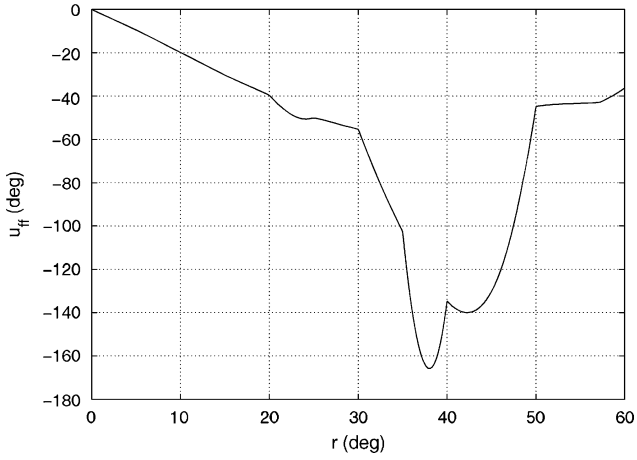

Fig. 9 Nonlinear feedforward function $[\phi_{ac}^{-1}(\bar{r})]$.

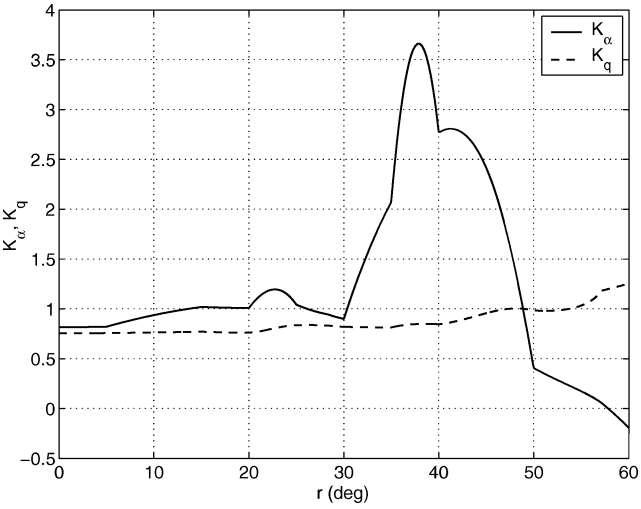

Fig. 10 $K_\alpha = \psi_{ac_\alpha}[\phi_{ac}^{-1}(r)]$ and $K_q = \psi_{ac_q}[\phi_{ac}^{-1}(r)]$ as scheduled functions of *r*.

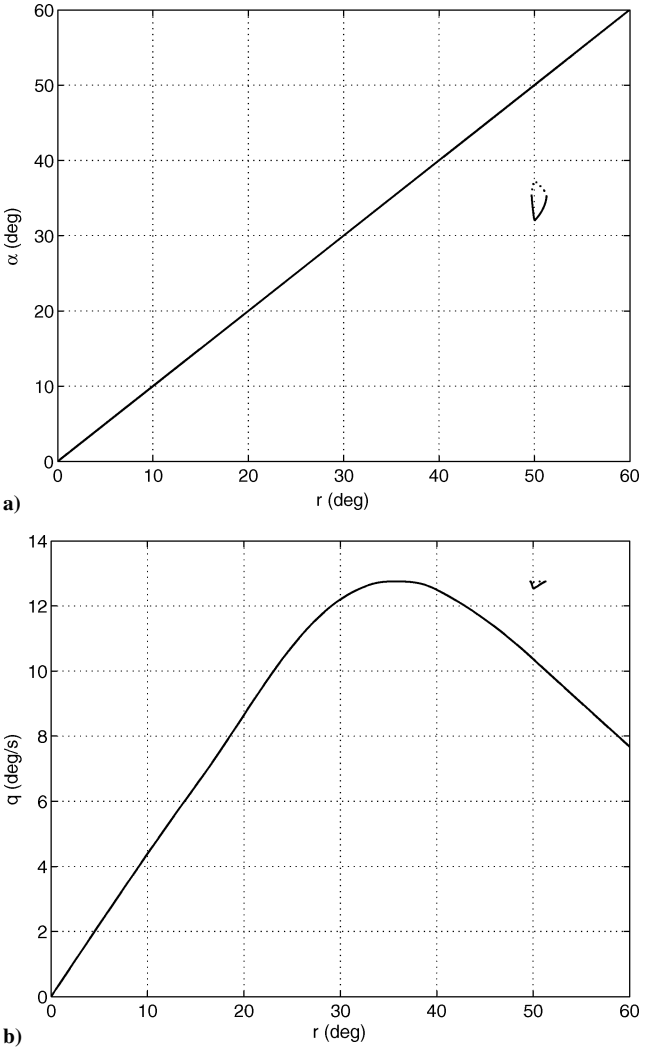

Fig. 11 Bifurcation diagrams: aircraft with feedforward and feedback control.

The bifurcation diagrams for the closed-loop system using the reference r as the continuation parameter are shown in Fig. 11. A branch can be seen denoting the desired linear relationship between r and α. The branch is stable; however, it is not unique. A small, isolated set of equilibria can be seen consisting of both stable and unstable equilibrium points. The existence of this set of unwanted equilibria demonstrates that a local control strategy can have global effects on the nonlinear system.

The bifurcation diagram defines the equilibria of the system, and as such, the eigenvalues relate to the trimmed (equilibrium) state of the aircraft.

In designing the controllers for this paper, feedback gains were only calculated at the trim points that satisfied the control requirement where $\alpha = r$. When only a feedforward term and feedback gains on the system states are used, additional attractors, stable and unstable, can still exist away from the desired branch. The implication is that the stability region around the desired branch of equilibria may be reduced in size, at least for some input values, to an extent that renders unacceptable behavior when transient responses take the system away from the local neighborhood of the desired equilibria. This type of control system cannot guarantee that the desired trim branch is unique.

The significant advantage shown here of using bifurcation analysis and continuation in the controller design is that the resulting global dynamics due to a locally designed controller can be investigated and assessed early in the design phase.

The closed-loop eigenvalues are shown in Fig. 5 for the desired stable branch over the α range 0–60 deg. These show that, as well as remaining stable, the aircraft model will exhibit the required level-1 handling qualities at every point on the desired set of equilibria. As mentioned, the response away from this trim branch for which the controller was designed will differ from the desired dynamics. This can be seen immediately by considering the effect of the isola, which consists of both stable and unstable equilibria.

Figure 12 shows the closed-loop HHIRM response to step changes in r with both the feedforward and the feedback schedules. Given a 15-deg step in r (Fig. 12a), the response in the output α is as predicted by the desired eigenvalues, that is, a damping ratio of

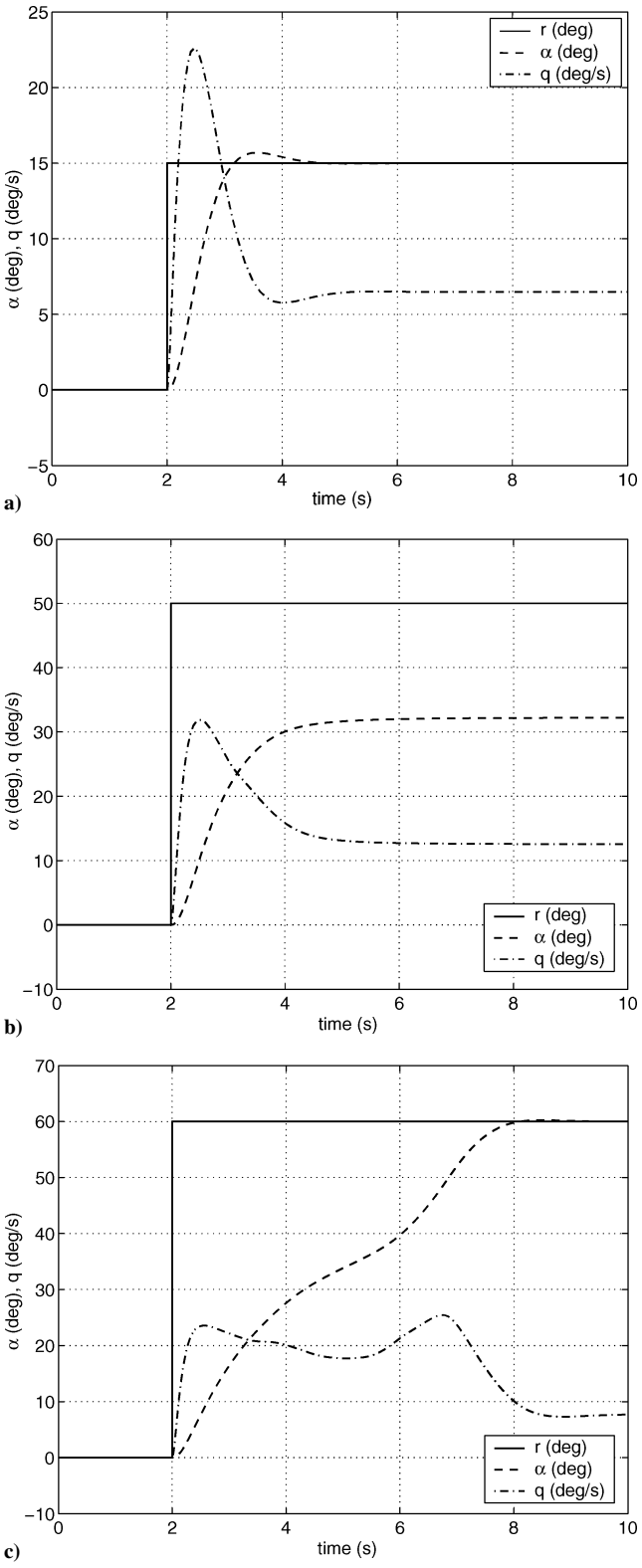

Fig. 12 HHIRM step response under feedforward and feedback control: a) 15-deg step, b) 50-deg step, and c) 60-deg step.

approximately 0.707, giving a single overshoot, and a settling time of approximately 2 s. This desired response is a reflection of the relatively linear region over which the step demand is made.

A step demand of 50 deg in r (Fig. 12b) places the system into the region of attraction created by the additional attractors shown in Fig. 11. This time, the aircraft settles onto the undesired stable attractor at $\alpha = 32.2$ deg, rather than the desired equilibrium lying at $\alpha = 50$ deg.

Furthermore, given a step input of $r = 60$ deg, even when the system does not end up on an undesired equilibria the trajectory in α clearly shows the influence of the extra attractor, despite there only being the one (desired) equilibria set in the system at $r = 60$ deg (Fig. 11). Thus, the isolated equilibria can be linked to changes in the global dynamic response and are shown to influence the trajectories in the surrounding state space.

VI. Bifurcation Surface Plots

Continuation methods as tools for control design can be extended to assess the effect that variation of the controller gains has on the closed-loop system. The controller gains themselves can be used as continuation parameters to map out a surface of equilibria from the open-loop to the closed-loop bifurcation diagram. Namely, we can assess the effect of varying the gains of a state feedback controller of the form $u = \boldsymbol{K}_{\text{fb}} x$.

Several surfaces could be made in terms of variation of each feedback gain individually. In this case, however, to demonstrate the technique we vary all of the gains simultaneously by introducing a new continuation parameter Λ and defining the feedback control as

$$u = \Lambda \boldsymbol{K}_{\text{fb}} \boldsymbol{x} \tag{30}$$

where $\boldsymbol{K}_{\text{fb}}$ is fixed as the set of controller gains designed using the eigenstructure assignment methods from the preceding section. In effect, Λ is a weight coefficient on the controller gains, or feedback scale factor: $\Lambda = 0$ indicates no feedback, that is, the open-loop system and $\Lambda = 1$ implies full feedback as designed using eigenstructure assignment.

Continuation is then carried out using Λ as the continuation parameter. Figure 13 shows the surface of equilibria for the second-order HHIRM model, with $0 \leq \Lambda \leq 1$. Exporting the data from the numerical continuation software (AUTO) to MATLAB® enables the surface to be easily manipulated as a three-dimensional plot.

In Fig. 13a, the flat surface corresponding to the desired set of equilibria at $\bar{\alpha} = \bar{r}$ can clearly be seen to exist for all values of Λ. This is as predicted in Sec. III.C: The feedforward term in the control ensures the existence of equilibria at $\bar{\alpha} = \bar{r}$ regardless of the feedback control. As shown earlier, though, these equilibria are not necessarily stable or unique.

The evolution of the surface as Λ increases can be seen more clearly in the contour plot of the surface (Fig. 13b). The loci of equilibria other than the $\bar{\alpha} = \bar{r}$ surface gradually reduce in size as Λ increases. From the open-loop system, the additional branches shrink as the influence of the feedback gains increases.

The unstable section of the desired trim branch also decreases as Λ increases until on either side of this main trim branch the two isola are formed. The isola above the desired trim branch in Fig. 13b disappears completely before Λ reaches 1.

Moreover, the surface confirms the existence of the additional equilibria shown in Fig. 11. These equilibria correspond to a peak in the surface of Fig. 13b persisting up to $\Lambda = 1$. This is more easily seen in Fig. 13c, the view parallel to the flat surface where $\bar{\alpha} = \bar{r}$. The significance of this peak is that, although the controller ensures a desired eigenstructure along a set of desired equilibria, it does not necessarily eliminate all unwanted equilibria.

The implication of this set of results is that the use of continuation methods in both design and analysis stages allows the global implications of a local controller to be identified. Hence, continuation methods can provide some measure of robustness of the control strategy under investigation. Specifically, bifurcation analysis can shed light on those topological changes in the system that may otherwise not be fully understood when using a more traditional approach to control system design. For example, when the existence and origin of the undesired isola have been identified, it is possible to take the analysis one stage further and to find the demands that need to be placed on this existing controller to obtain a single stable attractor. This can be done, as will be shown, by using Λ as the continuation parameter and finding the limit of the peak identified in the three-dimensional plot. The role that bifurcation analysis can play in control system design is currently the subject of much ongoing research (for instance, Ref. 10).

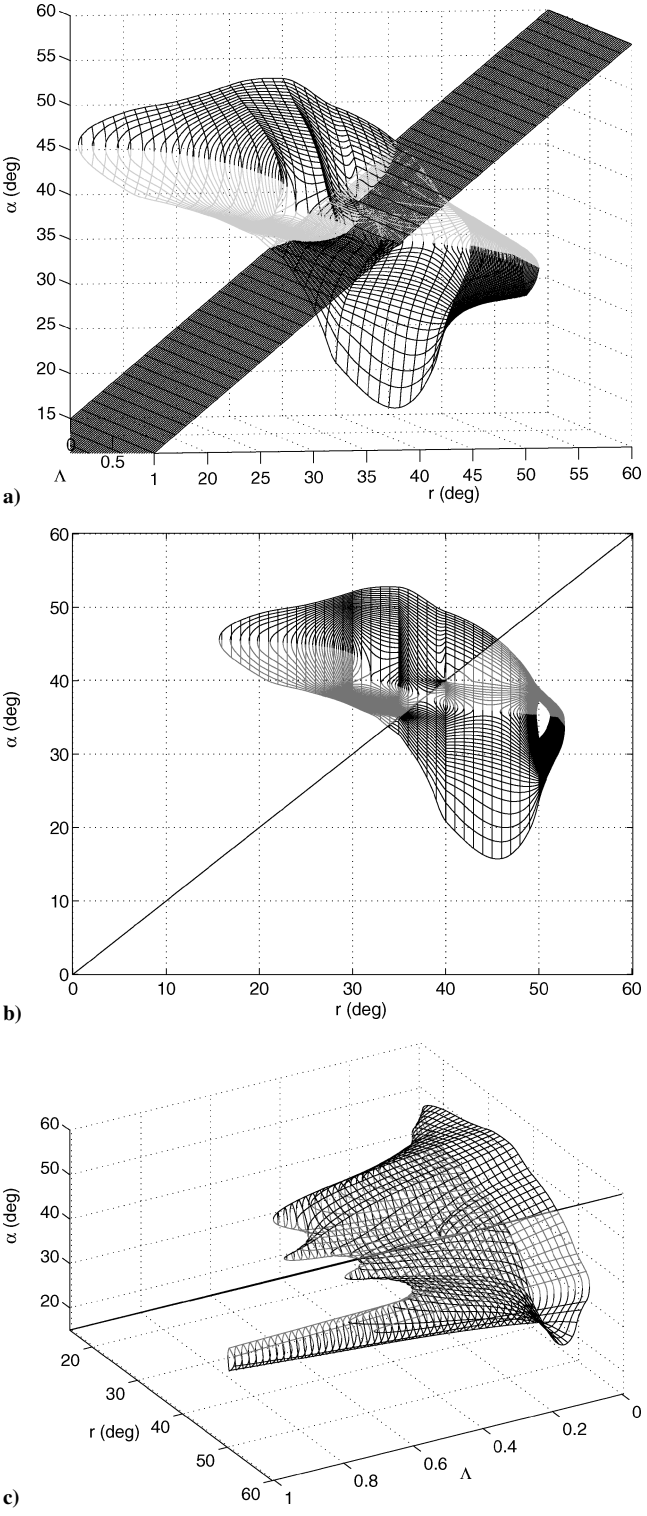

Fig. 13 Surface of equilibria for feedforward and feedback system: from zero feedback control ($\Lambda = 0$) to the full feedback control using gains designed using eigenstructure assignment ($\Lambda = 1$).

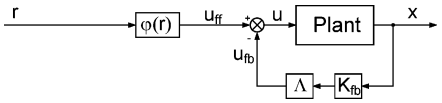

Fig. 14 State feedback plus feedforward control.

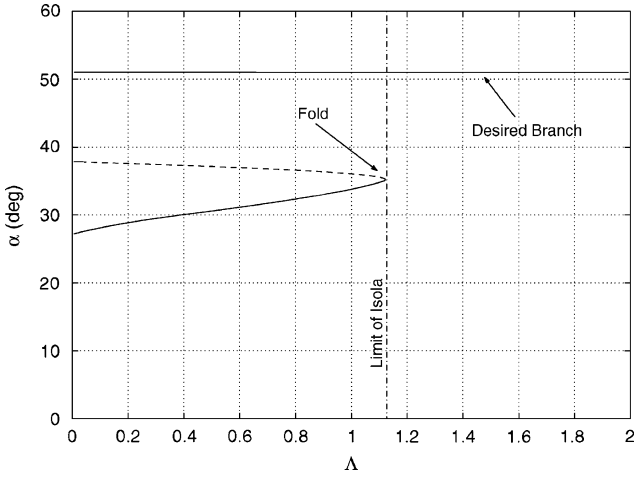

Fig. 15 Bifurcation digram: Λ = continuation parameter.

A. Continuation with Λ

We start by taking a point roughly at the center of the unwanted isola, $\alpha = 35$ deg; r is fixed at 51 deg. The continuation algorithm is set up to find steady states in α and q. To do this, u_{ff} has to be calculated at each point in the iteration.

Figure 14 shows the change that must be made to the system to use Λ as the continuation parameter. A constant value of u is selected that matches with the value of α at 51 deg. Given this value for u and the fact that the desired trim point is constant with α and q, then the feedback term varies only with Λ and it is possible to simplify the equation to give u_{ff} in terms of only Λ. Therefore u_{ff}, the input signal, is given by

$$u_{\text{ff}} = u^* + \Lambda\left(K_\alpha^* \alpha^* + K_q^* q^*\right) \tag{31}$$

where the asterisk denotes the value at the desired equilibria. The bifurcation diagram is shown in Fig. 15 and consists of two branches. A single, stable, horizontal branch is shown that corresponds to the desired set of equilibria at $\alpha = 51$ deg. The second branch has varying α and corresponds to the undesired isola shown in the earlier results. When this section is used, through the three-dimensional plots it is possible to indentify the limit of the isola (which arises via a fold bifurcation) and the values of Λ for which only the single desired attractor exists in the region under investigation.

From these results it can be seen that using $\Lambda = 1.2$ would give a system where only the single stable attractor would exist. An alternative to the continuation given here would be to carry out a local optimization in terms of r and α that would find the true local maximum of Λ. For the purposes of this paper, however, the results given by this continuation are sufficient to find a value of Λ that would give a single stable attractor. (An optimization approach has the disadvantage that it provides no insight into topological changes as the feedback scale factor varies.)

Figure 16 shows the eigenvalues for the closed-loop system with a single attractor between $\alpha = 0$ and $\alpha = 60$ deg, with $\Lambda = 1.2$. The resulting eigenvalues are no longer fixed over the α range, but have been moved to the left. The controller designer is now in a position to carry out a trade study between a system displaying ideal local equilibria with transient dynamics affected by the isola, or a system with compromised eigenstructure but benefitting from an enlarged stability region of the desired equilibria and, hence, no isola. In fact, in the HHIRM example, the damping and frequency of the system at $\Lambda = 1.2$ remain in the level-1 handling qualities range: It would be possible to redesign the controller with eigenvalues fixed in this region of the complex plane (instead of at $-2 \pm 2j$), which would also result in the isola being removed.

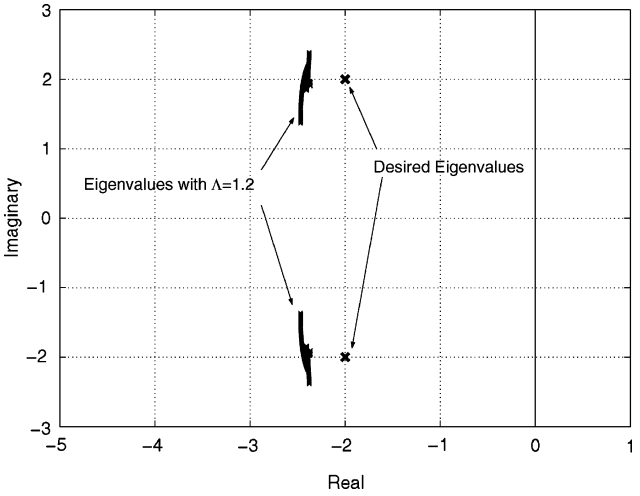

Fig. 16 Eigenvalues with Λ = 1.2.

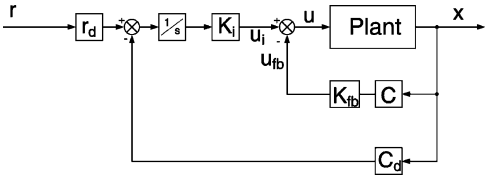

Fig. 17 Output feedback plus integral control.

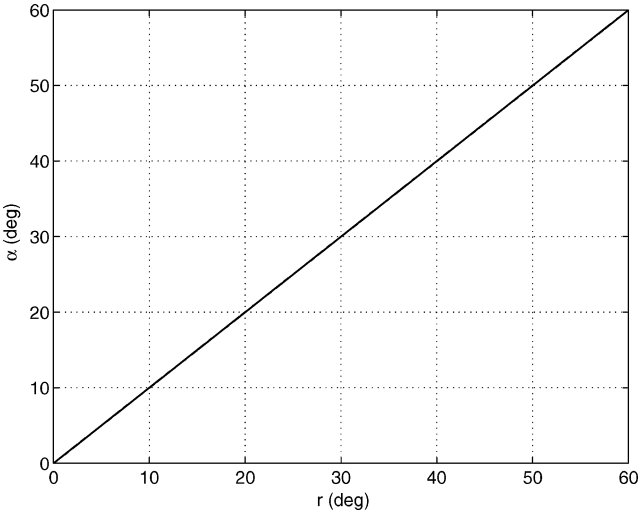

Fig. 18 Bifurcation diagram: closed-loop HHIRM with integral control.

B. Feedback Plus Integral Control

Figure 17 is a block diagram in which feedback control is used to alter the dynamic properties of the closed-loop system and integral control is used to generate a demanded response through the use of an outer demand loop. This configuration is more robust to changes in plant parameters and is an alternative method for removing the undesired isola.

Theoretically, assuming unlimited control power for the HHIRM and using the control structure shown in Fig. 17, only the single desired set of equilibria can exist. A note of caution must be added though because, even though there may not be a second stable attractor within the envelope considered, the region of attraction for the desired equilibria is not guaranteed to be global. A trajectory may exist that would take the system outside of the desired envelope, where the system may no longer be controllable.

Figure 18 is the bifurcation diagram for the gain-scheduled system with integral control. It is clear that only the desired stable set of equilibria exists, and the undesired isola is no longer present. Control surface position limits are not considered here, but the

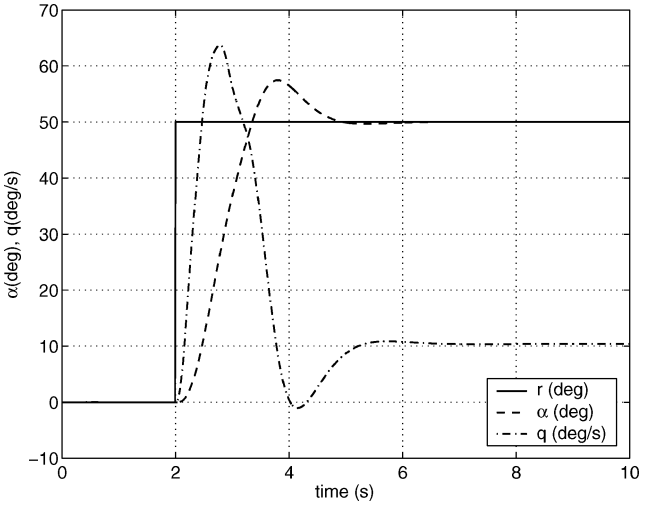

Fig. 19 Response of HHIRM with integral control to step of 50 deg in *r*.

continuation-based approach can also accommodate control surface saturation.[20]

As a result of the apparently unique equilibria branch in Fig. 18, it would be reasonable to expect a large stability region and, hence, that transient dynamics would show an improved response relative to that for the feedback plus feedforward control.

Figure 19 is the response of the closed-loop system to a step change in the reference r of 50 deg. This is a great improvement over the corresponding response shown in Fig. 12 with the system coming to rest at the desired 50 deg with dynamics corresponding to eigenvalues lying at $-2 \pm 2j$. The undesired isola is no longer present and, therefore, cannot have an effect on the surrounding phase space and transient response.

VII. Conclusions

A novel technique using continuation methods was presented in which surfaces of equilibria were formed for a highly nonlinear aircraft dynamic system with feedforward- and feedback-scheduled controller. Synthesis of the controller gains was embedded within the continuation method. The equilibrium surfaces were displayed graphically in terms of the controller gain variation and the reference signal. This allowed easy visualization of the effect of changing the control gains and the resulting global implications of the locally designed control strategy. Results were shown to include undesired attractors and transient responses. Where large parameter/input variations are involved in a nonlinear system, local analysis of controllers may prove insufficient. The technique presented here provides a tool to aid the understanding of the global dynamics and allows global stability to enter the controller design studies.

These results show that there is great benefit in a logical and practical approach to control system design that helps to evaluate the global implications of a locally designed controller. The combination of gain-scheduled control with nonlinear analysis methods is demonstrated to be a practical way of addressing complex problems of this type.

Acknowledgments

The provision by QinetiQ Ltd., Bedford, England, U.K., of the hypothetical high angle of incidence research aircraft model is gratefully acknowledged.

References

[1]Carroll, J., and Mehra, R., "Bifurcation Analysis of Nonlinear Aircraft Dynamics," *Journal of Guidance, Control, and Dynamics*, Vol. 5, No. 5, 1982, pp. 529–536.

[2]Lowenberg, M., "Bifurcation Analysis of Multiple-Attractor Flight Dynamics," *Philosophical Transactions of the Royal Society A: Mathematical, Physical and Engineering Sciences*, Vol. 356, Oct. 1998, pp. 2297–2319.

[3]Mehra, R., and Carroll, J., "Global Stability and Control Analysis of Aircraft at High Angles of Attack," Technical Rept. ONR-CR215-248-3, Scientific Systems Inc., Cambridge, MA, June 1979.

[4]Seydel, R., "Assessing Voltage Collapse," *Latin American Applied Research*, Vol. 31, No. 3, 2001, pp. 171–176.

[5]Barnett, W., and He, Y., "Analysis and Control of Bifurcations in Continuous Time Macroeconomic Systems," *Proceedings of IEEE Conference on Decision and Control*, Inst. of Electrical and Electronics Engineers, New York, 1998, pp. 2455–2460.

[6]Mehra, R., Kessel, W., and Carroll, J., "Global Stability and Control Analysis of Aircraft at High Angles of Attack," Technical Rept. ONR-CR215-248-1, Scientific Systems Inc., Cambridge, MA, June 1977.

[7]Rugh, W., and Shamma, J., "Research on Gain Scheduling," *Automatica*, Vol. 36, No. 10, 2000, pp. 1401–1425.

[8]Goman, M., Khramtsovsky, A., and Usoltev, S., "High Incidence Aerodynamics Model for Hypothetical Aircraft," Technical Rept. 15/5DRA, Defense Research Agency, Bedford, Bedfordshire, England, U.K., Nov. 1995.

[9]Stevens, B., and Lewis, F., *Aircraft Control and Simulation*, Wiley, New York, 1992, pp. 107–116.

[10]Chen, G., Yu, X., and Hill, D. (eds.), *Chaos and Bifurcation Control: Theory and Applications*, Springer-Verlag, Berlin, 2003, pp. 249–264.

[11]Strogatz, S., *Nonlinear Dynamics and Chaos: with Applications to Physics, Biology, Chemistry and Engineering*, Addison–Wesley, Reading, MA, 1994, pp. 15–92.

[12]Mönnigmann, M., and Marquardt, W., "Bifurcation Placement of Hopf. Points for Stabilization of Equilibria," *Proceedings of International Federation of Automatic Control (IFAC)*, International Federation of Automatic Control, Laxenburg, Austria, 2002.

[13]Glendinning, P., *Stability, Instability and Chaos: An Introduction to the Theory of Nonlinear Differential Equations*, Cambridge Univ. Press, Cambridge, England, U.K., 1994, pp. 222, 223.

[14]Doedel, E., and Wang, X., "AUTO94: Software for Continuation and Bifurcation Problems in Ordinary Differential Equations," California Inst. of Technology, Center for Research on Parallel Computing, Technical Rept. CRPC-95-2, Pasadena, CA, 1995.

[15]Richardson, T., Davison, P., Lowenberg, M., and di Bernardo, M., "Control of Nonlinear Aircraft Models Using Dynamic State-Feedback Gain Scheduling," AIAA Paper 2003-5503, Aug. 2003.

[16]Andry, A., Shapiro, E., and Chung, J., "Eigenstructure Assignment of Linear Systems," *IEEE Transactions on Aerospace and Electronic Systems*, Vol. 19, No. 5, 1983, pp. 711–728.

[17]Hodgkinson, J., *Aircraft Handling Qualities*, AIAA, Reston, VA, 1999, pp. 58, 59.

[18]*A Background to the Handling Qualities of Aircraft*, Engineering Sciences Data Unit, London, Data Item 92006, 1992, p. 23.

[19]Hsu, C. S., *Cell-to-cell Mapping: A Method of Global Analysis for Nonlinear Systems*, Springer-Verlag, Berlin, 1987, pp. 1–30.

[20]Richardson, T., Stoten, D., Lowenberg, M., and Bernardo, M., "Continuation Methods for Aircraft Models Subject to Integrator Wind-Up," AIAA Paper 2004-4946, Aug. 2004.